Regional synthesis and mapping of soil organic carbon and nitrogen stocks at the Canadian Beaufort coast

Julia Wagner [1,2], Juliane Wolter[3,4], Justine Ramage[1,2], Victoria Martin[5], Andreas Richter[5], Niek Jesse Speetjens[6], Jorien E. Vonk[7], Rachele Lodi[8,9], Annett Bartsch[10], Michael Fritz[4], Hugues Lantuit[4,11], and Gustaf Hugelius[1,2]

[1]Department of Physical Geography, Stockholm University, Stockholm, Sweden
[2]Bolin Centre for Climate Research, Stockholm, Sweden
[3]Institute of Biochemistry and Biology, University of Potsdam, Potsdam, Germany
[4]Alfred Wegener Institute Helmholtz Centre for Polar and Marine Research, Potsdam, Germany
[5]Centre for Microbiology and Environmental System Science, University of Vienna, Vienna, Austria
[6]School of Environmental Studies, University of Victoria, Victoria, BC, Canada
[7]Department of Earth Sciences, Vrije Universiteit Amsterdam, Amsterdam, Netherlands
[8]National Research Council (CNR), Institute of Polar Sciences, Venice, Italy
[9]Department of Environmental Sciences Informatics and Statistics, Ca' Foscari University of Venice, Venice, Italy
[10]b.geos GmbH, Korneuburg, Austria
[11]Institute of Geosciences, University of Potsdam, Potsdam, Germany

Correspondence: Julia Wagner (julia.wagner@natgeo.su.se)

Abstract. Permafrost soils are particularly vulnerable to climate change. To assess and improve estimations of carbon (C) and nitrogen (N) budgets it is necessary to accurately map soil carbon and nitrogen in the permafrost region. In particular, soil organic carbon (SOC) stocks have been predicted and mapped by many studies from local to pan-Arctic scales. Several studies have been carried out at the Canadian Beaufort Sea coast, though no regional synthesis of terrestrial carbon stocks based on spatial modelling has been conducted yet. This study synthesises available field data from the Canadian coastal plain and uses it to map regional SOC and N stocks using the machine learning algorithm random forest and environmental variables based on remote sensing data. We explore local differences in soil properties and how soil data distribution across the region affects the accuracy of the predictions of SOC and N stocks. We mapped SOC and N stocks for the entire region and provide separate models for the coastal mainland area and Qikiqtaruk Herschel Island. We assessed performance of different random forest models by using the Area of Applicability (AOA) method. We further applied the quantile regression forest method to the mainland and Qikiqtaruk Herschel Island models for SOC stocks and compared the results with the AOA method. Our results indicate that not only the selection of data is crucial for the resulting maps, but also the chosen covariates, which were picked by the models as most important. The estimated SOC stock for the upper metre is 56.7 ± 5.6 kg m^{-2} and the N stock 2.19 ± 0.51 kg m^{-2}. The average SOC stocks vary significantly when including or excluding data in the predictive models. Qikiqtaruk Herschel Island is geologically different from the coastal mainland and has lower SOC stocks. Including Qikiqtaruk Herschel Island soil data to predict SOC stocks at the mainland has large impact on the results. Differences in N stocks were not as dependent on the location as SOC stocks and rather differences between individual studies occurred. The results of the separate models show 36.2 ± 5.7 kg C m^{-2} and 2.66 ± 0.39 kg N m^{-2} for Qikiqtaruk Herschel Island and 57.2 ± 4.5 kg C

m^{-2} and 2.17 ± 0.50 kg N m^{-2} for the mainland. Our results diverge from previous studies of lower resolution, showing the
20 added regional-scale accuracy and precision that can be achieved at intermediate resolution and with sufficient field data.

1 Introduction

The northern Permafrost region, which is approximately 22% of the earth's surface (Obu, 2021), is considered vulnerable to
climate change. With air temperatures rising up to four times faster than the global average (Meredith et al., 2022; Rantanen
et al., 2022), permafrost is thawing across the pan-arctic. Between 2017 and 2016 permafrost temperatures in the continuous
25 permafrost zone have increased by 0.39 ± 0.15 °C (Biskaborn et al., 2019). The permafrost region contains ca.1,600 Gt
of carbon, including ca.1000 Gt stored in frozen ground, which is twice as much as atmosphere (Strauss et al., 2021). The
thickening of the active layer, driven by warming, increases carbon availability for decomposition, releasing greenhouse gases
like carbon dioxide and methane, which further amplify climate warming. This is called the permafrost-climate feedback
(Schuur et al., 2015). In addition to gradual thaw, ice-rich permafrost is particularly prone to thermokarst and abrupt thaw
30 events (Turetsky et al., 2020) which further accelerate losses of permafrost carbon.

Approximately one third of the earth's coastlines are Arctic (Lantuit et al., 2012) and coastal permafrost areas are especially
prone to changes. Average coastal retreat rates of -0.7 m yr^{-1} (Irrgang et al., 2018) were detected along the Yukon coast. This
represents considerable changes, taking into account that previous studies estimated SOC fluxes of 132 kg C yr^{-1} per metre
of shoreline from land to sea at the Yukon coast (Couture et al., 2018b). Therefore, it is crucial to estimate soil organic carbon
35 (SOC) and nitrogen (N) stocks in the coastal lowland area. The study area is characterised by extensive ice-wedge polygon
(IWP) terrain, high ground ice content and the occurrence of thermokarst.

Quantification and mapping of SOC using different methods have been carried out on pan-Arctic (Hugelius et al., 2014;
Mishra et al., 2021) and local level (Obu et al., 2017; Palmtag et al., 2018; Siewert et al., 2015, 2016; Siewert, 2018; Wag-
ner et al., 2023). However, few studies have investigated how the shift from local to regional scale affects accuracy and the
40 prediction results. The availability of intermediate to high resolution datasets for larger areas in recent years (e.g. Bartsch
et al., 2019a; Widhalm et al., 2019) offers the possibility to investigate local and regional SOC and N stocks using the same
data and therefore connects the different scales. As permafrost soil properties and ice content are highly variable, especially
in ice-wedge polygon (IWP) terrain (e.g. Siewert et al., 2021a), high-resolution studies that represent the variability at the
pedon-scale of <2 m (e.g. Wagner et al., 2023), the terrain scale (ranging up to tens of metres) up to landscape scale are needed.
45 The variability at landscape scale can now be represented in pan-Arctic studies such as Mishra et al. (2021) with a resolution
of 250 m or better. Studies in between those scales are lacking, but necessary when quantifying regional carbon budgets. While
Couture et al. (2018b) studied fluxes from nearshore terrain units, our study is the first for the region that combines all available
terrestrial SOC and N data to predict regional SOC and N stocks.

A range of different methods have been used to upscale permafrost SOC stocks, including landcover class upscaling (e.g.
50 Obu et al., 2017; Palmtag et al., 2018). Machine learning (ML) algorithms are also widely used for the spatial mapping of SOC
and N stocks (e.g. Siewert, 2018; Wagner et al., 2023), or for investigating C and N fluxes (Virkkala et al., 2024). Machine

learning as part of digital soil mapping (DSM) generates model based datasets for soil properties. Based on the "SCORPAN"-principle (McBratney et al., 2003) covariates representing the soil forming factors (soils, climate, organisms, terrain, parent material, age, spatial location) are identified and spatial patterns and relationships between those and the target variable are used to predict the target variable to the whole area (Lagacherie, 2008). Next to geostatistical methods, machine learning methods are the current state of the art, especially recommended to map permafrost soils due to the spatial heterogeneity and the ability of ML to detect non-linear relationships (Siewert et al., 2021a). A method that is suitable for evaluating the representativeness of predictive models is the area of applicability (Meyer and Pebesma, 2021). The AOA method computes a dissimilarity index (DI) by analysing the relationship between the target variable and covariates in prediction areas, accounting for variable importance and location distances. Areas poorly represented by these relationships receive a low DI, and a threshold is used to classify regions into applicable or non-applicable areas. To quantify regional C and N budgets, quantifications of soil C and N stocks are necessary. The aim of this study is to quantify SOC and N stocks and their local-scale variability in the whole lowland area at the Yukon coastal plain. The targeted spatial resolution is 10 m.

To reach this overall aim, the specific objectives of our study are

(1) to synthesise research on SOC and N stocks that has been carried out in the study region,

(2) to provide regional spatial datasets of SOC and N stocks and

(3) to assess our predictions via the area of applicability (AOA) method, to quantify the uncertainty with quantile regression forest and to discuss the importance of considering local heterogeneity in the data.

2 Material and methods

2.1 Study area

The study area is located in the continuous permafrost zone (Obu et al., 2019) of the Yukon Coastal Plain and comprises the coastal lowland area below 180 m.a.s.l. and Qikiqtaruk Herschel Island (in further description named as Herschel Island) (Fig 1A). During the Last Glacial Maximum (LGM) the study area was partially glaciated with the Laurentide ice sheet reaching up until west of Herschel Island during the Wisconsinan glaciation (Fritz et al., 2011; Rampton, 1982). Herschel Island represents a unique feature, namely an ice-thrust moraine created by the advance of the Laurentide ice sheet (Fritz et al., 2012; Rampton, 1982). Rampton (1982) mapped the quaternary deposits of the region. The western area, outside of the LGM glacial limit, is composed of mainly lacustrine deposits. Colluvial slopes are found in areas with higher elevation and greater distance from the coast. The area within the former glacial limits is composed by lacustrine and outwash plains. The whole area is transected by several rivers flowing towards the Arctic Ocean, creating alluvial fens, floodplains and stream terraces. Further, some areas are rich in organic material with peat layers of 0.4 to 3.5m thickness.

The study area is high in ground ice, with an average of 46% volume of ground material and up to 74% in some areas (Couture and Pollard, 2017; Couture et al., 2018b). The study area is highly prone to erosion with mean coastal erosion rates of - 0.7 $\mathrm{m\,yr^{-1}}$, with some parts eroding up to 9 $\mathrm{m\,yr^{-1}}$ (Irrgang et al., 2018). On Herschel Island several well-studied retrogressive thaw slumps occur and retreat rates of $0.45 \pm 0.48 \, \mathrm{m\,yr^{-1}}$ between 1970 and 2000 (Lantuit and Pollard, 2008) and

85 $0.68 \pm 2.48 \, \mathrm{m \, yr^{-1}}$ between 2000 and 2011 were estimated (Obu et al., 2016). The local scale landforms in the study area are determined by permafrost and ground ice with large areas covered by IWP tundra. The formation and geomorphology of these IWP systems has been extensively studied (e.g. Fritz et al., 2016; Wolter et al., 2016, 2018). Another commonly occurring landform feature are drained thermokarst lake basins (DTLB) which are subject of current studies due to their potential for carbon storage (Wolter et al., 2024). The climate is characterised as Tundra climate. Between 1972 and 2000, mean annual

90 temperatures were -9.9 °C and -11.0 °C at the nearby weather stations Komakuk Beach and Shingle point, respectively. During the summer months (June, July and August) average temperatures of 8.6 C (±1.7 °C) at Shingle point and 6.0 °C (±1.6 C) at Komakuk Beach were observed (Government of Canada, 2024). The active layer depths in the study area reported in the literature range from 30 to up to 50 cm (Siewert et al., 2021a; Wagner et al., 2023; Wolter et al., 2018). The vegetation close to the coast is characterised by tussock and non-tussock sedge, dwarf-shrub, moss tundra and sedge, moss, dwarf-shrub and low

95 shrub wetlands. Herschel Island is defined by erect dwarf-shrub tundra (Walker et al., 2005).

2.2 Synthesis and processing of soil data and predictor variables

This study focuses on coastal lowland tundra and Herschel Island, the mapping region (Fig. 1A) was selected from the DEM by using areas with an elevation below 180 m. This threshold includes all the area of Herschel Island, while not expanding too far inland where soil data is limited.

100 Soil property data was retrieved from existing publications (Table 1, Fig. 1), harmonised and converted into the depth intervals 0-30 cm and 30-100 cm. The studies were conducted with different sampling designs and goals, causing spatial clustering of data points in the study area. The studies by Siewert et al. (2021a) and (Ramage et al., 2019) both followed a transect approach, the study by Obu et al. (2017) sampled representative sites per ecological unit and Couture et al. (2018a) sampled sites along the coast. Wagner et al. (2023) followed a stratified random sampling approach. The study by Siewert et al.

105 (2021a) focuses on soil properties at a small scale and contains values for subpedons which are soil profiles in 10 cm intervals generated from 1 metre wide transects. Such a high level of detail was not necessary in our study. Therefore these values were averaged per pedon.

In addition to published data, new data from DTLBs that were sampled during a field campaign in April 2019 was added to this synthesis. The DTLB data covers drained lake basins between Herschel Island and Kay Point at different distances

110 inland from the coast (0.6-14.0 km) and on various elevations (3-65 m), with one central coring location per basin. We cored 24 frozen sediment cores using a SIPRE permafrost corer during this campaign. We aimed to core at least the top metre of sediment including active layer and permafrost and reached 88-200 cm sediment depth, except for core YC19-DTLB-17 (88 cm) and YC19-DTLB-20 (95 cm). All cores were kept frozen until subsampling and analysis. We described core stratigraphies and subsampled all cores at 5 cm resolution or according to stratigraphic boundaries. The stratum of the drainage event was

115 sampled in 2 cm resolution. We weighed the frozen soil samples and measured their dimensions to calculate sample volume. We then calculated water contents as the difference before and after freeze drying, and calculated dry bulk densities as dry sample weight divided by wet sample volume. We analysed freeze dried ground samples for total organic carbon (TOC) content using

an Elementar Soli TOC® cube, and for total nitrogen (TN) content using an Elementar Rapid Max N exceed analyser. All analyses were conducted at laboratories of the Alfred Wegener Institute of Polar and Marine Research in Potsdam, Germany.

120   The predictor variables used in the study were taken from published datasets at a spatial resolution of 10 - 20 m (Table 2). All raster datasets were resampled to 10 m and reprojected to the UTM coordinate system (EPSG code 32607). The landcover data (Bartsch et al., 2019b) was converted into binary variables and the dominating classes in the area were selected. Those were "dry to moist prostrate to erect dwarf shrub tundra" (LC_class4) and "moist to wet graminoid prostrate to erect dwarf shrub tundra" (LC_class5). Uncertainties may need to be considered regarding the role of landcover. The representation of

125 landcover strongly depends on the used spatial resolution. (Bartsch et al., 2024) applied super-resolution processing based on a convolutional neural networks approach to the 20m bands of Sentinel-2. In the resulting 10m version, re-assignment reflected the high heterogeneity. The largest differences in unit assignment occurred for the shrub tundra groups which are dominating along the Canadian Beaufort Sea coast. Our study uses the 20m product, as the 10m product was not available yet when the analysis was completed.
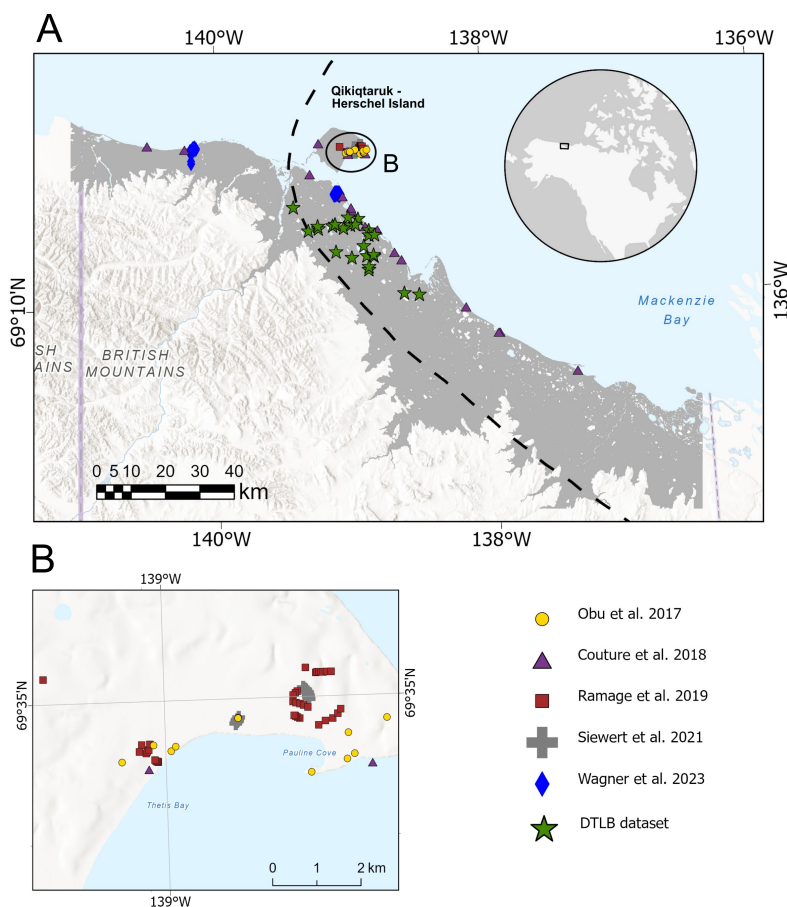
Figure 1. Overview of the study area, locations and sources of the soil data used in this study (A) and zoom-in to the eastern part of Herschel Island (B). The DTLB dataset is a new dataset previously unpublished and included in this study (for more information see chapter 2.2). The mapping extent is shown in grey on top of the Basemap: ESRI (2024a).

2.3   Random forest mapping, area of applicability and uncertainty

This study focuses on creating spatial predictions individually for the mainland and Herschel Island (Fig. 1), creating a separate model that combines all data and comparing the results of the models. All analysis were carried out in R studio using R version 4.1.2 (R Development Core Team, 2021). The random forest algorithm (Liaw and Wiener, 2002) implemented in the package caret (Kuhn, 2008, 2022) was used for mapping SOC and N stocks for the whole area as well as with separate models for Herschel Island and mainland the coastal area. Random forest is a decision-tree based algorithm that builds a large amount of trees based on bootstrap samples of the training data and aggregating their results. This process aims to reduce the prediction error and is also called "bagging" (bootstrap and aggregating). The number of trees (ntree), the amount of covariates selected

Table 1. Overview of the datasets, their sources, aim of the study and availability of SOC and N stock data.

Datasource	SOC stock data Available	N stock data Available	Location	Aim of the study
Obu et al. (2017) (Paper) Obu et al. (2016) (Dataset)	yes	yes	Herschel Island	Upscaling of SOC and N stocks
Couture et al. (2018a) (Paper) (Couture et al., 2018a) (Dataset)	yes	no	Herschel Island and along the Yukon coast	Mapping SOC and N stocks and fluxes along the Yukon coastal plain
Ramage et al. (2019) (Paper+Dataset)	yes	yes	Herschel Island	SOC and N stocks along Hillslopes in three valleys
Siewert et al. (2021a) (Paper) Siewert et al. (2021b) (Dataset)	yes	no	Herschel Island	Mapping of small scale Variations in SOC
Wagner et al. (2023) (Paper) Wagner et al. (2024) (Dataset)	yes	yes	Two representative catchments at the Yukon coast	Mapping of SOC and N stocks
DTLB dataset	yes	yes	Drained thermokarst lake basins at the Yukon coast	Thorough investigation of drained lake basins, SOC and N data published here

at each split (mtry) and the minimum amount of training data to continue splitting the tree (nodesize) can be manually defined (Breiman, 1996, 2001).

140   The "boruta" algorithm (Kursa and Rudnicki, 2010) was used for feature selection prior to the training of the random forest models. The algorithm was run with random forest, a maximum repetition of 2500 and a maximum of 1500 trees. The Boruta algorithm serves as a wrapper algorithm and assesses the significance of predictors by contrasting their importance with their corresponding shadows, discarding those with notably lowered importance. These shadows mirror the initial variables, featuring randomly shuffled values while maintaining the original distribution and are regenerated in each iteration. The algorithm
145   stops either as soon as reaching the maximum of specified runs or when only the attributes considered important remain (Kursa and Rudnicki, 2010). Separate random forest models were trained for the depth 0-30 and 30-100 cm for the whole study area including all data. Additional models were trained for Herschel Island and the mainland using the respective data. The reason for creating separate models and predictions was due to Herschel Island being an ice thrust moraine (Rampton, 1982) and therefore geologically very different from the coastal mainland area. The mtry was chosen by grid search where RMSE was
150   the lowest. Mtry is the amount of variables chosen at each split (Liaw and Wiener, 2002). The internal validation was set to

Table 2. Overview of the predictor variables, their sources, spatial resolution, acronym used, and brief description.

Variable	Data Source	Spatial resolution	Acronym	Description
Elevation	ArcticDEM (Porter et al., 2018)	10m	DEM	Digital surface model
Landcover data	Bartsch et al. (2019b)	20m	LC	Landcover derived from Sentinel 1 and 2 data
NDVI (Normalised Difference Vegetation Index)	Bartsch et al. (2024)	10m	NDVI	Based on Sentinel 2
NDWI (Normalised Difference Water Index)	Bartsch et al. (2024)	10m	NDWI	Based on Sentinel 2
NDBI (Normalised Difference Built-up Index)	Bartsch et al. (2024)	10m	NDBI	Based on Sentinel 2
Vegetation height	Bartsch et al. (2019a)	20m	VH	Vegetation height derived from Sentinel 1 and 2 data
Normalised C-VV winter backscatter	Bartsch et al. (2024)	10m	S1 C VV	Based on Sentinel 1
Normalised C-HH winter backscatter	Widhalm et al. (2019)	20m	S1 C HH	Based on Sentinel 1

10-fold crossvalidation repeated 20 times for all models, except two where leave-one-out crossvalidation was chosen due to a low amount of datapoints. Ntree was set to 500 and nodesize was kept at its default value of 5. We provide the internal validation results: mtry at which the best performing model was selected according to the lowest RMSE, R2 (fraction of %), mean absolute error (MAE), the number of predictors (n pred), the number of samples (n samp) and StDev. Additionally, we
155 display for simplicity the first three important variables (short: var) for each model, var1, var2 and var3 (Table 4).

To further evaluate the prediction, the "area of applicability" – method (Meyer and Pebesma, 2021) implemented in the package CAST version 0.9.0 (Meyer et al., 2024) was applied to each model. The area of applicability (AOA) estimates the area where the application of the predicted model is likely accurate and lies within the prediction error (RMSE). The AOA is based on the dissimilarity index (DI) which is calculated based on the minimum distance to the training data within
160 the multidimensional predictor space, where predictors are weighted with respect to their importance in the model prior to the distance calculation. Then a threshold to the DI is applied which is the maximum DI of the training data obtained via crossvalidation resulting in a binary raster layer with 1 representing the AOA and 0 displaying areas outside the AOA. In addition to the AOA we used quantile regression forest as described by Yigini et al. (2018) and also applied by (Wagner et al., 2023) to estimate the uncertainty which includes the sensitivity of the model to available data and the uncertainty of the model.
165 We applied this workflow to the mainland and Herschel Island models for the carbon stocks.

3 Results

3.1 Data synthesis of regional carbon and nitrogen stocks

The individual studies included in this synthesis showed a large variety in their distribution of SOC stocks (Fig. 2). Stocks were generally lower on Herschel Island (Fig. 2) compared to the mainland, mirroring geological differences. All the studies carried out solely on Herschel Island showed lower SOC stock values, with the study by Ramage et al. (2019) having the lowest values in the depth increments 0-30 and 30-100 cm with averages of 10.2 and 16.1 kg m^{-2} respectively. The study by Siewert et al. (2021a) showed the highest average values with 16.0 and 29.6 kg m^{-2} and the study by Obu et al. (2017) was in between with average values of 11.9 and 26.8 kg m^{-2}. The studies carried out on the mainland showed average values of 17.6 and 31.2 kg m^{-2} (DTLB dataset) and 21.5 and 42.6 kg m^{-2} (Wagner et al., 2023). The study by Couture et al. (2018b) used sites on Herschel Island as well as coastal sites on the mainland, so the average values were higher than on Herschel Island and in a similar range to the mainland studies at 18.6 and 26.6 kg m^{-2}.

Table 3. Mean, median, standard deviation (StDev) and number of datapoints per study used in this synthesis.

study	SOC stocks [kg m^{-2}] 0-30 cm				SOC stocks [kg m^{-2}] 30-100 cm			
	mean	median	StDev	N	mean	median	StDev	N
Couture et al. 2018	18.6	16.0	6.9	17	26.6	26.5	11.2	17
Obu et al. 2017	11.9	10.4	7.7	12	26.8	24.5	19.5	12
Ramage et al. 2019	10.2	10.0	3.8	43	16.1	16.0	7.2	43
Siewert et al. 2021	16.0	15.5	4.0	38	29.6	31.0	11.0	38
Wagner et al. 2023	21.5	21.0	8.1	83	42.6	41.7	16.6	83
DTLB dataset	17.6	18.1	4.9	18	31.2	30.2	8.2	18

study	N stocks [kg m^{-2}] 0-30 cm				N stocks [kg m^{-2}] 0-30 cm			
	mean	median	StDev	N	mean	median	StDev	N
Couture et al. 2018	NA	NA	NA	0	NA	NA	NA	0
Obu et al. 2017	0.84	0.90	0.43	12	2.45	2.60	1.36	12
Ramage et al. 2019	0.79	0.80	0.22	43	1.35	1.35	0.47	43
Siewert et al. 2021	NA	NA	NA	0	NA	NA	NA	0
Wagner et al. 2023	1.21	1.19	0.51	83	2.48	2.46	1.00	82
DTLB dataset	0.74	0.71	0.28	10	1.68	1.70	0.36	10

In contrast, N stocks showed a different pattern with higher N stocks at the sites of the studies by Obu et al. (2017) and Wagner et al. (2023), especially in the depth 30-100 cm compared to the datasets by Ramage et al. (2019) and the DTLB dataset (Fig. 2 and Table 3). After dividing SOC and N values between 'mainland' and 'Herschel Island, average SOC stock

180 values were 13.0 kg m^{-2} in depth 0-30 cm and 23.1 kgm^{-2} at 30-100 cm for Herschel Island and 20.6, while average SOC stock values for the mainland were 38.9 kg m^{-2}. The N stocks on Herschel Island were 0.8 and 1.59 kg m^{-2} and 1.16 and 2.39 kg m^{-2} on the mainland (Fig. 2). The distribution further shows that mean and median values are close (Fig. 2).

3.2 Random Forest mapping and model validation assessment

The models for the whole area who R^2 values of 0.24 and 0.17 for the SOC stocks and 0.2 and 0.19 for the N stocks. When
185 separated, the models for the mainland had the lowest R^2 values of 0.11 and 0.10 for the SOC stocks and R^2 values of 0.17 and 0.18 for the N stocks (Tab. 4). The models for the SOC stocks at Herschel Island had an R^2 value of 0.28 for 0-30 cm and 0.35 for 30-100 cm. The RMSE values of all models were below the standard deviation (StDev) of the distribution of the data values The highest values for SOC and N stocks are predicted in the areas close to the coast with lower values with increasing distance from the coast (Fig. 3). The average SOC stocks (Table 5) for the models using all data for the whole area were 14.9
190 kg m^{-2} at 0-30 cm and 29.5 kg m^{-2} at 30-100 cm depth. The N stocks were 0.90 and 0.91 kg m^{-2} respectively. When both SOC and N stocks, were modelled separately for Herschel Island and the mainland, higher SOC and N stocks were modelled on the mainland and lower SOC and N stocks on Herschel Island. The only exception to that were N stocks on Herschel Island for 30-100 cm depth (Table 5). SOC stocks at 0-30 cm depth were 19.9 kg m^{-2} for the mainland and 12.2 kg m^{-2} for Herschel Island, when both areas were modelled separately, in contrast to using the all data for the whole area, which resulted in an
195 average of 14.9 kg m^{-2} (Table 5).

The elevation was the most important predictor variable driving the distribution of SOC and N stocks for all models over the whole area (Table 4, Fig. 4). While figure 4 shows examples of two variable importance plots, the variable importance for the remaining models is shown by figures S1 and S2 (supplement). The most important variable for the mainland was the normalised difference water index (NDWI) for all models, except the SOC stocks at 30-100 cm depth, where landcover class 4
200 ["dry to moist prostrate to erect dwarf shrub tundra"] was more important in determining the distribution of SOC stocks. The models for Herschel Island determined different variables as most important, with elevation and landcover class 4 being the most important for the SOC and N stocks at 0-30 cm depth respectively. The NDWI and vegetation height were most important in the models for SOC and N stocks at 30-100 cm depth.
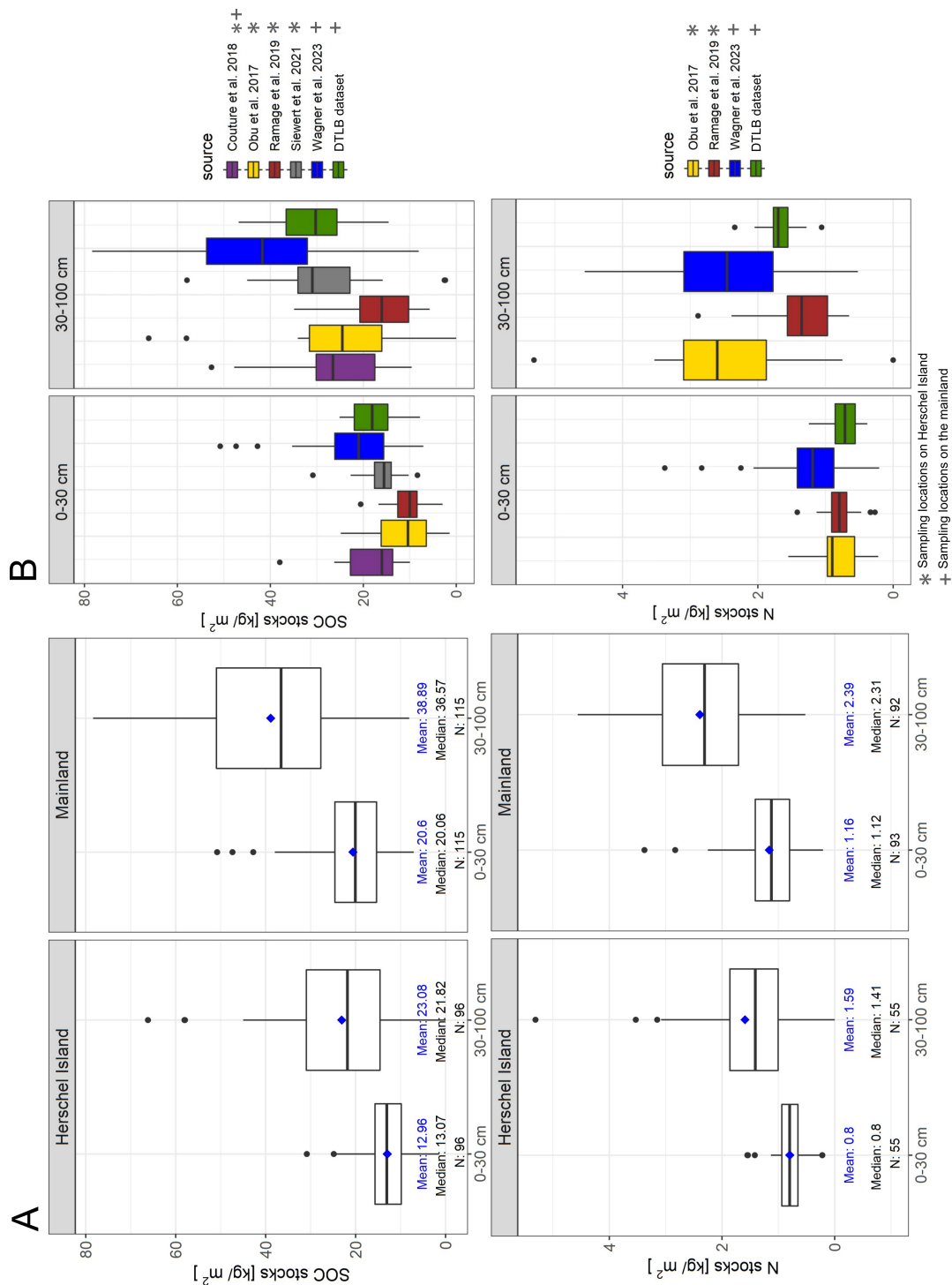
Figure 2. Soil organic carbon (SOC) and nitrogen (N) stocks per depth interval separated into mainland and Herschel Island (A) and per study area (B).

3.3 Area of Applicability (AOA) and uncertainty with quantile regression forest

205 The analysis of the DI and AOA showed that areas where models were not reliable are mostly located around streams and lakes, as well as higher elevation areas further away from the coast (Fig. 5 and Fig. 6). The analysis also shows that a large area on Herschel Island, where no samples are available, had a high DI, limiting the applicability of the model. Generally, areas that are too different from the sampled areas had a high DI and are outside the AOA. However, sites with similar sample-predictor relations to the sampled sites, but further away, were still suitable and within the AOA (Fig. 6). In models using all data and

210 the models for the mainland, predicted SOC and N stock values inside the AOA were generally higher (for example 20.9 ± 2.8 kg C m^{-2} inside the AOA compared to 19.9 ± 2.8 kg C m^{-2} for the mainland model at 0-30 cm depth; Table 5). For Herschel Island there was no difference between AOA and whole area.

The results of the quantile regression forest uncertainty (Fig. S3 and S4, supplement) showed areas around lakes and streams as having high uncertainty, similar to the AOA analyses. At Herschel Island (Fig. S4, supplement) the highest uncertainty

215 is towards the coast, in depressions and near streams. The area in the centre of Herschel Island, that has been identified as inapplicable by the AOA method, has contrastingly a lower uncertainty measured by the quantile regression forest.
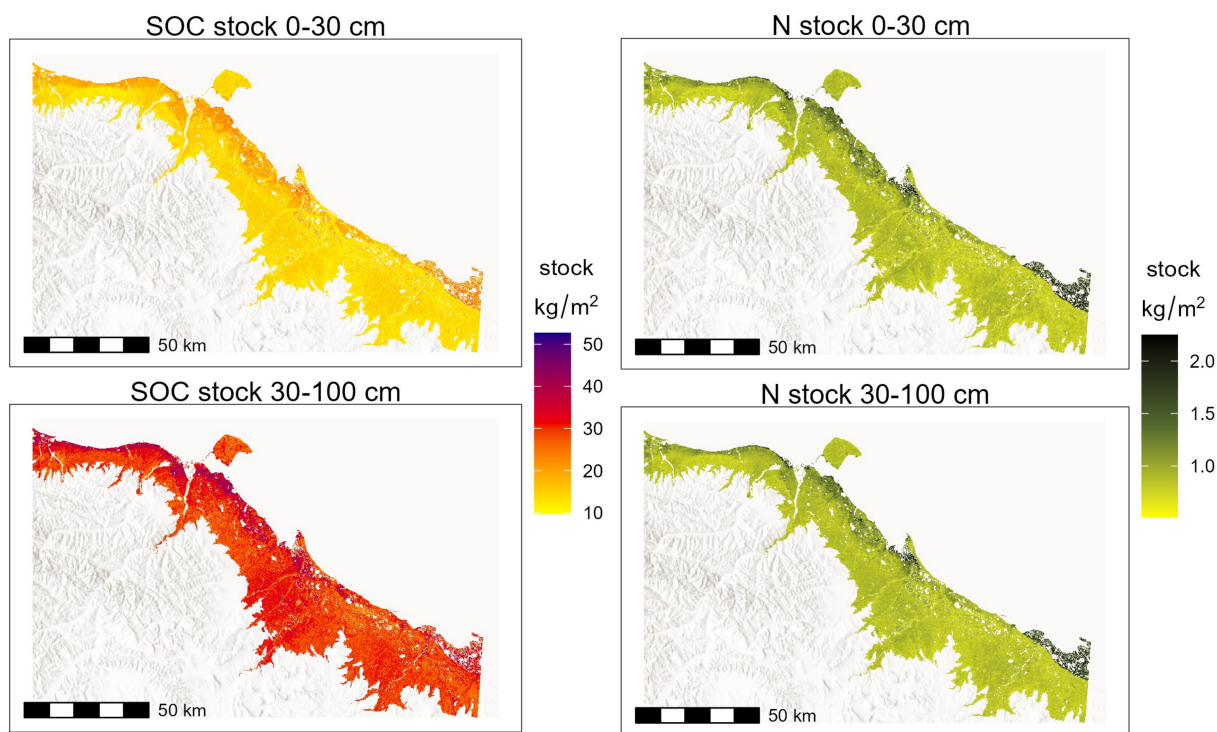
Figure 3. Prediction of soil organic carbon (SOC) and nitrogen (N) stocks for the whole study area using all data (Basemap: ESRI (2024b)).
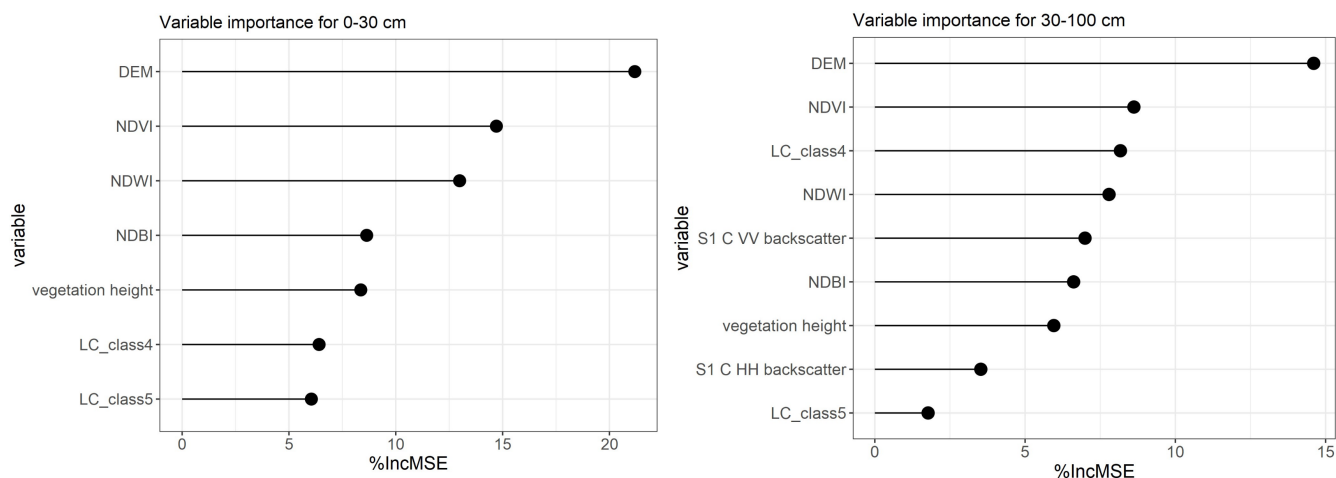
Figure 4. Variable importance for the models predicting soil organic carbon (SOC) for the whole area in depth 0-30 and 30-100 cm. For the variable importance for all models see supplement. (variables: DEM=digital elevation model, NDVI= Normalised Difference Vegetation Index, NDWI= Normalised Difference Water Index, NDBI= Normalised Difference Built-up Index, vegetation height, LC_class4= dry to moist prostrate to erect dwarf shrub tundra, LC_class4= moist to wet graminoid prostrate to erect dwarf shrub tundra, S1 C VV backscatter= Normalised C-VV winter backscatter from Sentinel-1, S1 C HH backscatter= Normalised C-HH winter backscatter from Sentinel-1).

Table 4: Results of the random forest models. The table shows the internal validation results: mtry at which the best performing model was selected according to the lowest RMSE. R2 (fraction of %), mean absolute error (MAE), the number of predictors (n pred), the number of samples (n samp) and StDev are displayed together with the first three important variables for each model (Var1, Var2 and Var3). The table continues on the next page.

model	mtry	RMSE	R2	MAE	StDev	n pred	n samp	validation method	Var1	Var2	Var3
whole area											
SOC stock 0-30 cm	2	6.86	0.24	5.23	7.80	7	189	10-fold CV, repeated 20 times	DEM	NDVI	NDWI
SOC stock 30-100 cm	2	15.30	0.17	11.99	16.43	9	189	10-fold CV, repeated 20 times	DEM	NDVI	LC_class4

N stock 0-30 cm	2	0.46	0.20	0.33	0.49	4	135	10-fold CV, repeated 20 times	DEM	NDWI	NDBI
N stock 30-100 cm	2	0.46	0.19	0.34	1.02	5	135	10-fold CV, repeated 20 times	DEM	NDWI	NDVI
mainland											
SOC stock 0-30 cm	2	7.59	0.11	5.83	7.74	9	107	10-fold CV, repeated 20 times	NDWI	NDVI	veg height
SOC stock 30-100 cm	2	17.12	0.10	13.99	16.04	9	107	10-fold CV, repeated 20 times	LC_class4	NDWI	NDVI
N stock 0-30 cm	2	0.48	0.17	0.36	0.51	4	93	10-fold CV, repeated 20 times	NDWI	NDBI	DEM
N stock 30-100 cm	2	0.48	0.18	0.36	0.98	5	93	10-fold CV, repeated 20 times	NDWI	NDBI	NDVI
Herschel Island											
SOC stock 0-30 cm	2	4.86	0.28	3.75	5.28	7	78	10-fold CV, repeated 20 times	DEM	NDBI	NDVI

SOC stock 30-100 cm	2	10.58	0.35	8.30	12.60	7	78	10-fold CV, repeated 20 times	NDWI	veg height	NDBI
N stock 0-30 cm	2	0.23	NA	0.23	0.30	9	42	leave-one-out CV	LC_class4	NDBI	NDVI
N stocks 30-100 cm	2	0.74	NA	0.74	0.87	9	42	leave-one-out CV	veg height	S1 C VV backscatter	NDBI
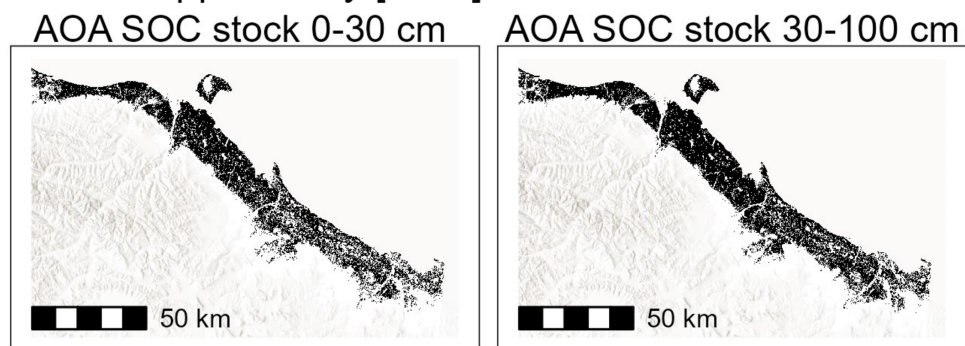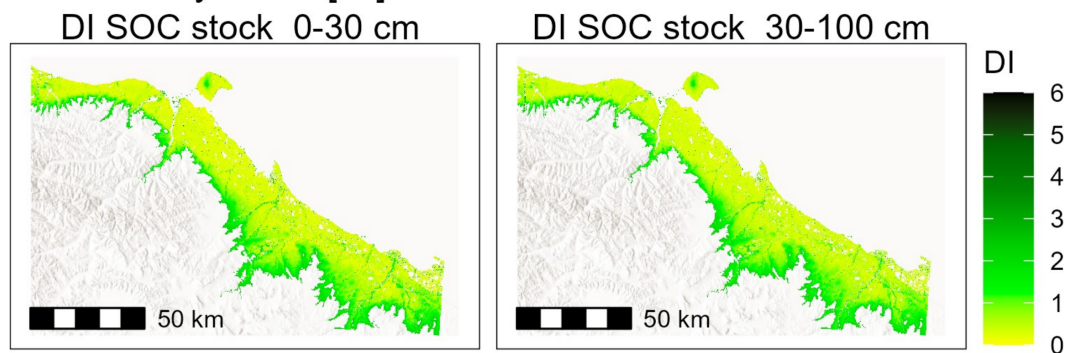
Figure 5. Area of applicability (AOA) and dissimilarity index (DI) for the predictive model of SOC stocks for the whole area. For DI thresholds that determine AOA see supplement (Tab. S1) (Basemap: ESRI (2024b)).
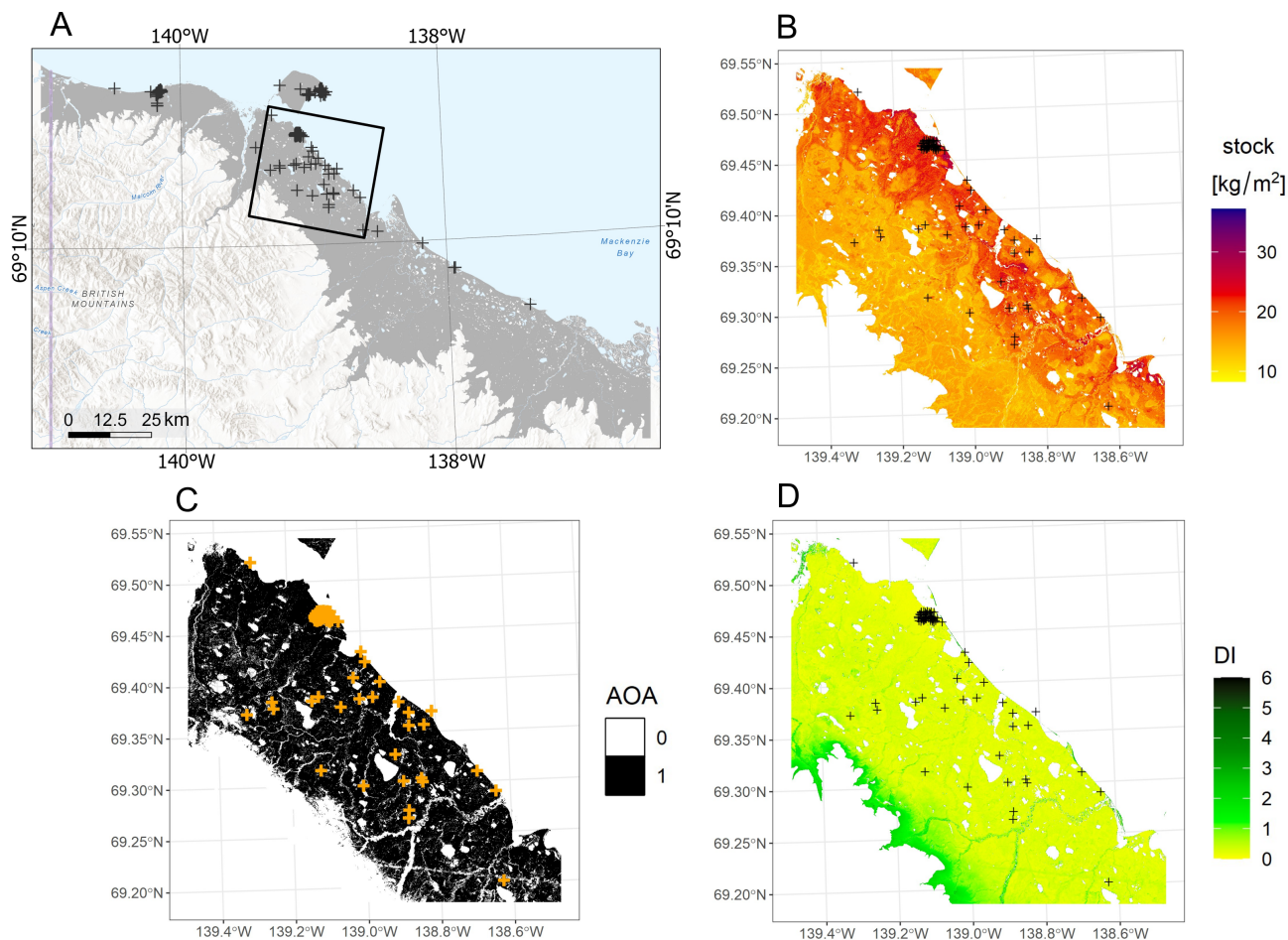
Figure 6. Zoom-in to an area (A, black square) with SOC stock distribution for depth 0-30 cm (B) the respective area of applicability (C) and dissimilarity index (DI). The datapoints are shown with cross symbols (Basemap in A: ESRI (2024a)).

Table 5. Comparison of average soil organic carbon (SOC) and nitrogen (N) stocks for each model prediction depicting the whole area and additionally the AOA of each respective prediction and predictive model (For more descriptive statistic values see supplement Table S2).

Prediction	SOC stocks 0-30 cm [kg/ m2]		SOC stocks 30-100 cm [kg/ m2]		N stocks 0-30 cm [kg/ m2]		N stocks 30-100 cm [kg/ m2]	
	mean	StDev	mean	StDev	mean	StDev	mean	StDev
whole area	14.9	3.0	29.8	4.3	0.90	0.23	0.91	0.21
whole area only AOA	16.2	3.6	30.6	5.1	0.97	0.27	0.98	0.26
mainland	19.9	2.8	37.3	3.3	1.08	0.26	1.09	0.25
mainland area only AOA	20.9	2.8	37.7	3.6	1.21	0.36	1.20	0.33
Herschel Island	12.2	1.7	24.0	4.7	0.83	0.11	1.83	0.32
Herschel Island only AOA	12.2	1.8	23.8	4.7	0.83	0.11	1.81	0.33
Herschel Island (from mainland prediction)	20.5	1.8	38.1	4.0	1.02	0.18	1.05	0.18
Herschel Island (from whole area prediction)	14.3	1.9	27.6	4.5	0.88	0.13	0.88	0.11
mainland (from whole area prediction)	14.9	3.0	29.9	4.3	0.90	0.23	0.91	0.21

4 Discussion

This study has significantly improved the data availability and knowledge about SOC and N stocks for the region. This new data compilation provides a benchmark dataset for further studies in the region, but also high-lights large remaining uncertainties.

220 4.1 Data synthesis of regional carbon and nitrogen stocks

Our study shows that already at a regional level there is a very high heterogeneity in field data, challenging the predictive ability of models. The full range of the available data in regional, but also in pan-Arctic synthesis must be representative for the entire study area. Data collection and sampling strategies from local studies are often tailored to a specific research question. This poses the risk that some landscape features may be over- and others underrepresented in the available data. It is therefore 225 advisable to analyse the values of the target variable at the sampling locations and the diversity of the landscape to ensure that

the spatial variability in the landscape is reflected by the sampled sites The AOA method can be used to assess whether the heterogeneity of the landscape, ideally mirrored in the covariates, is captured by the sampling locations. Areas where this is not the case can be excluded from regional estimates and could be further used to determine new sampling sites for future field sampling campaigns.

230   Our synthesis shows that SOC and N stocks are lower at Herschel Island than at the mainland (Fig. 2). This is likely due to Herschel Island being an ice thrust moraine (Rampton, 1982) and therefore being geologically different to the mainland. When looking at the studies individually, large differences occur even when comparing the studies only carried out on Herschel Island (Fig. 2). This is attributed to the different aims of the studies and site selection. While Obu et al. (2017) covered representative sites for different ecological units on Herschel Island, Ramage et al. (2019) sampled hillslopes in three valleys which show
235   significant levels of erosion. Erosive relocation of organic material which explains why SOC and N stocks are lower compared to the other studies. Siewert et al. (2021a) sampled representative sites in three typical ecological units on Herschel Island: hummocky tussock tundra, non-sorted circle tundra and IWP tundra. The selective sampling of specific representative areas was to study multi-scale variation of SOC distribution in specific permafrost landforms. The sites did not undergo significant erosion/ degradation and therefore SOC stocks are higher than at the sites of Ramage et al. (2019) and slightly higher than
240 Obu et al. (2017). The latter covers also moderately and strongly disturbed sites which show lower amounts of SOC are found in the upper soil (0-30 cm) as well as in the whole profile of 1 metre. Wagner et al. (2023) studied two typical small coastal catchments with dense sampling density. Particularly the sampling sites at Ptarmigan Bay were located in areas of high organic layer thickness (Rampton, 1982). The DTLB samples were exclusively from organic rich deposits (peat above lake sediment).

4.2   Spatial mapping of carbon and nitrogen stocks with random forest, area of applicability and uncertainty

245 Our analysis shows a substantial challenge in bridging from local- to regional-scale study areas. Already at the pedon scale permafrost soils are very heterogeneous (Siewert et al., 2021a), and this variability is retained in analyses at coarser scale. The m^{-2} values (Table 4) of the models of the entire area range from 0.17 to 0.24 which shows the predictive model can explain a 5th up to a quarter of the spatial heterogeneity in SOC and N stocks and the relationship between the data and the covariates at 10 m resolution. In contrast, the models for the mainland show even lower R^{-2} values ranging from 0.11-0.18. The models
250 for Herschel Island have higher R^2 values for the SOC stocks than the models for the entire area with 0.28 and 0.35. This may indicate that the variability in SOC could be better represented by the predictor variables at Herschel Island than at the mainland, but the difference may also be caused by less natural soil variability or a better representation of the soil data on Herschel Island.

    For Herschel Island, there was a higher data density (0.8 samples per km^2; n=78 for SOC, area approximately 108 km^2)
255 than on the mainland (0.02 samples per km^2; n=107 for SOC stocks, area approximately 4465 km^2). This has likely affected the accuracy of the models and may explain why mainland models have a lower R^2 values. It is also possible that the exact data density is less important than the spread and representation of the data in relation to natural variability between landscape types. Several of the studies on Herschel Island included representative sampling of multiple ecological units on the island, ensuring a range of landscape types are well characterised by the data.

260   The local heterogeneity in SOC and N stock distribution is also evident when different data are used to predict SOC stock distributions. Figure 7 displays the SOC stock distribution for the whole study area when using only data from the mainland (Fig. 7a and Fig. 1b), in contrast to training a model that also includes data from Herschel Island (Fig. 8 2a and 2b). When using all data, including Herschel Island, SOC stocks are lower, with averages of 14.9 kg C m^{-2} and 29.9 kg C m^{-2} for 0-30 and 30-100 cm depth, respectively. This is in large contrast to using only data derived from the mainland where SOC stocks

265   are considerably higher, with 19.9 kg C m^{-2} and 37.3 kg C m^{-2}. An opposing pattern is displayed in figure 8, where using all data results in higher SOC stocks at Herschel Island in comparison to using Herschel Island data only. The map with the largest SOC stocks is produced when interpolating from mainland data to Herschel Island (Fig. 8 2a and 2b).
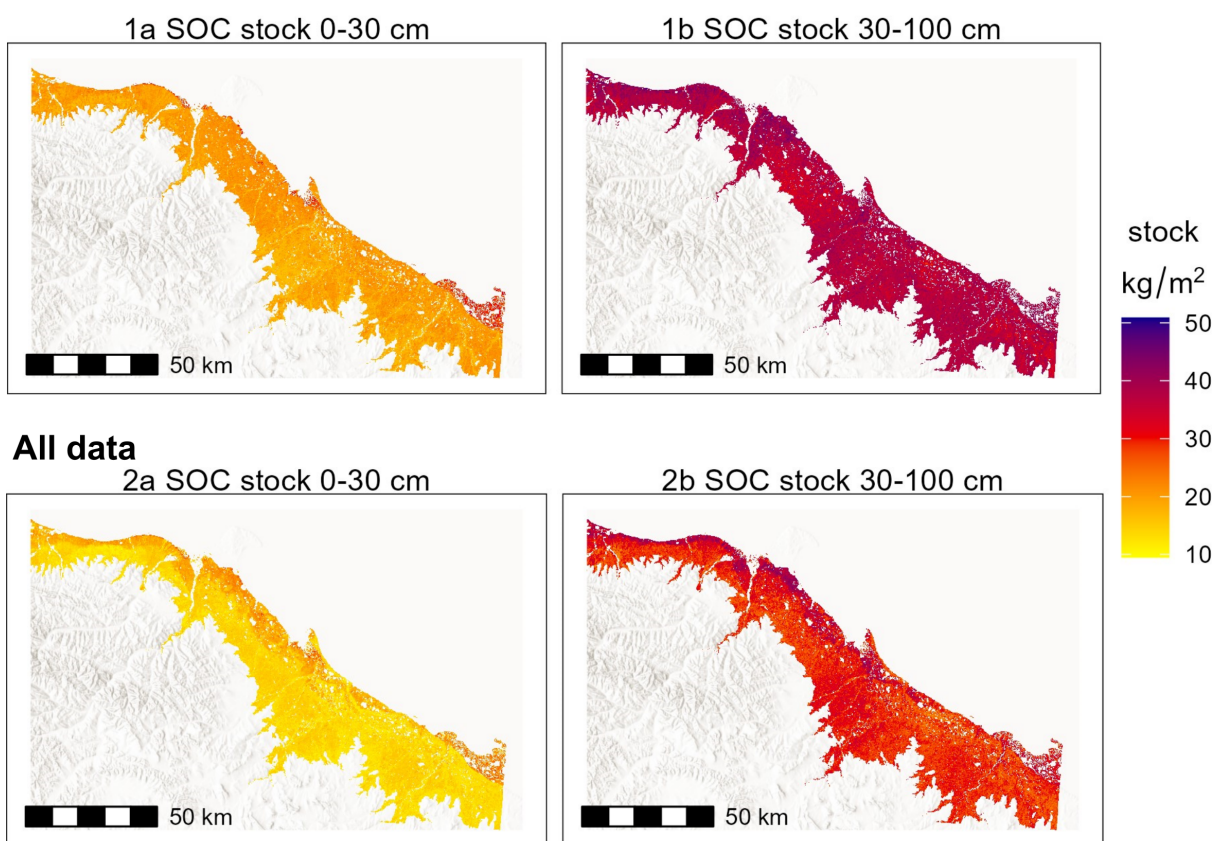
Figure 7. Comparison of soil organic carbon (SOC) stock for the coastal mainland region using only the mainland data (1a and 1b) and using all data (2a and 2b) (Basemap: ESRI (2024b)).

This analysis shows that the selection of data is crucial for studies at a regional scale. Data representation and potential site biases are also likely to be important for pan-Arctic SOC and N assessments. Mishra et al. (2021) carried out spatial

270   predictions for three regions separately: the North American, the Eurasian and the Tibetan Permafrost region. Our study shows

that differences in SOC stocks are significant even when comparing adjacent local scale areas. As the exclusion or inclusion of certain data has the potential to significantly influence in SOC/ N stock predictions, a more detailed differentiation, e.g. through geological units or terrain characteristics, would be recommended.
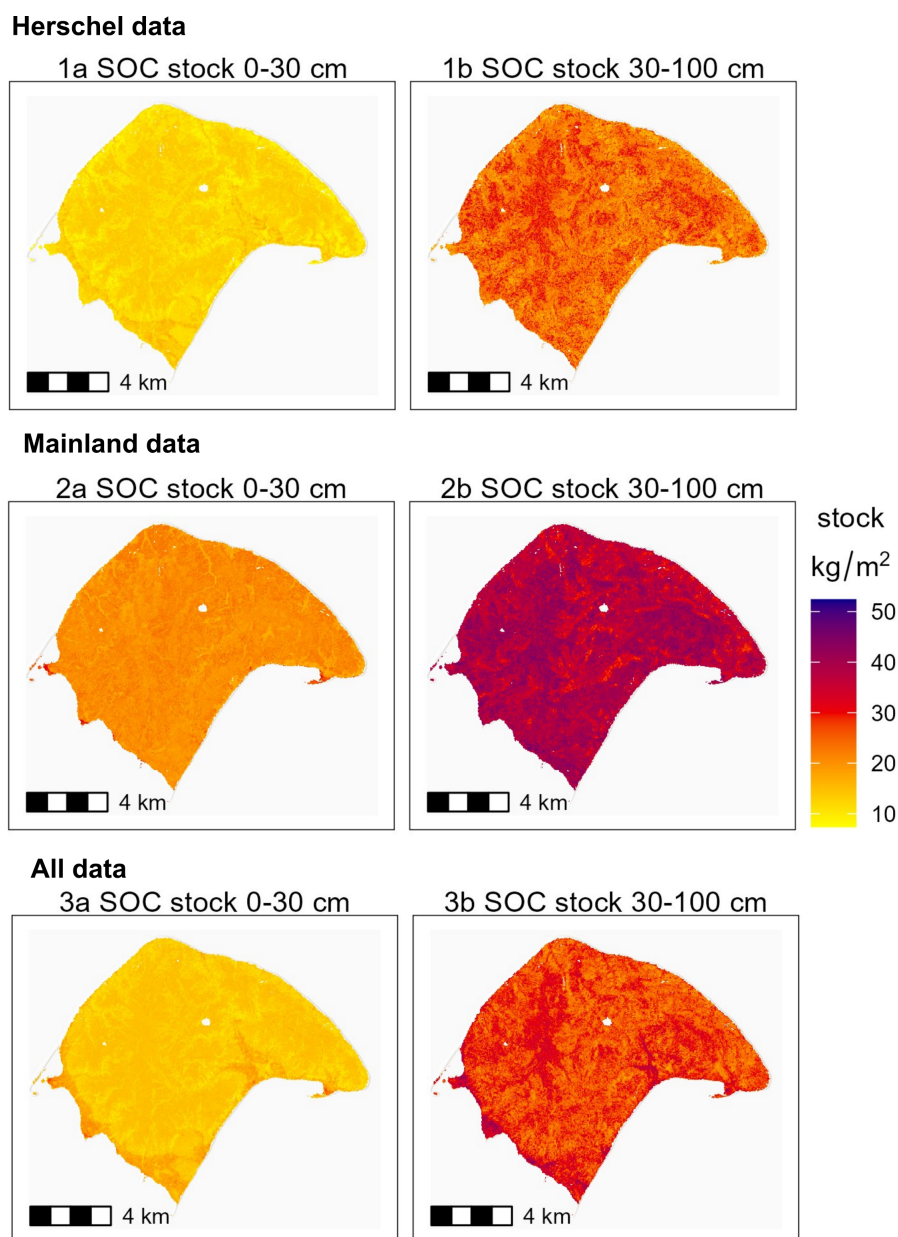
Figure 8. Comparison of soil organic carbon (SOC) stocks at Herschel Island using only datapoints on Herschel Island (1a and 1b), predicting (extrapolating) SOC only based on data from the mainland (2a and 2b) and using da for the entire area (3a and 3b) (Basemap: ESRI (2024b)).

Herschel Island in comparison to the mainland, especially the area in close proximity, is particularly interesting, since
275 soil forming factors such as landscape age, climate and vegetation are very similar, however the parent material differs. The
area at Ptarmigan Bay consists mostly of glaciofluvial and rolling moraine deposits (Rampton, 1982)). In contrast Herschel
Island consists of massive ground ice later buried by marine sediments (Burn, 2012). These differences in parent material
offer different conditions for soil development as their texture and geochemical composition differ. Studies show that carbon
enrichment through cryoturbation differs with grain size leading to higher carbon enrichment in higher coarse silt to very fine
280 sand fractions (Palmtag and Kuhry, 2018).

An assessment of uncertainty and model representation is crucial in digital soil mapping. Hugelius et al. (2014) used upscal-
ing of SOC stocks based on thematic maps representing the physiography and provide an uncertainty assessment in their study
that includes a "representation error" in the regions with lower data density. Similar considerations should be incorporated
in pan-Arctic studies that use DSM approaches such as machine learning models. The data used in synthesis studies might
285 be highly clustered and can show a high variability on regional and local level. This phenomenon is discussed by Meyer and
Pebesma (2022), mentioning that geographic clusters of the data do not necessarily mean gaps in the feature space, i.e. the
sample – predictor relationships may still represent the entire area.

To assess whether the presented models of our study are applicable for the total study area, we used the AOA method (Meyer
and Pebesma, 2021). It is expected that the dry areas of riverbeds and areas around lakes on the mainland are excluded after
290 applying the AOA, because these areas do not contain any sampling sites. Areas with larger distance from the coast were not
extensively sampled and therefore DI rises with distance from the coast. An interesting result in the AOA analyses is that
the model is not applicable to a large area in the centre of Herschel Island. The AOA method excludes this area likely due
to elevation differences that are not mirrored by the sampling locations. The AOA method includes consideration of variable
importance and DEM elevation most the important variable for the Herschel Island models (Table 4). The average SOC and
295 N stocks were slightly higher compared to the initial prediction when excluding not applicable areas. This shows that the
predictions outside the AOA are at the lower end of the spectrum of predicted values (Table 5). We believe that values that are
not represented by AOA are more likely to be underpredicted than overpredicted when using random forest for our study area.

The AOA method focuses on the relationship between covariates and data. We also applied the quantile regression forest to
the mainland and Herschel Island models for SOC stocks to assess uncertainty. This method estimates uncertainty from two
300 sources: the model itself and variations in the data. Data uncertainty is assessed by repeatedly applying a random forest model
to different datasets, while model uncertainty is calculated using quantile regression forests, and both are combined into a final
uncertainty map (Yigini et al., 2018). For the mainland models some areas of high DI overlap with high uncertainty (Fig. S5,
supplement). The Herschel Island models show high uncertainty in some areas with high DI, such as streams and depressions
near streams, but also low uncertainty in the centre where DI is high (Fig. S4, supplement). The quantile regression forest
305 method focuses on the uncertainty on a pixel basis. Multiple model runs are used to assess the sensitivity of the model to
available data and quantile regression forest is used to calculate a probability distribution for the values each pixel can take on.
In contrast, the AOA method assesses the applicability based on a certain model and the importance of the variables. To best

assess the accuracy of the predictions, we recommend using not exclusively one of the two methods, as the results may differ as was seen for Herschel Island in our study.

310   The selection of the covariates also significantly impacts the prediction power of models. Many studies in digital soil mapping in general (e.g. Hengl et al., 2017) but also pan-Arctic studies (Mishra et al., 2021) include parameters derived from digital elevation models such as slope, curvature, aspect, flow direction, flow accumulation, etc. Coastal lowland tundra areas generally have very flat terrain and are close to sea level, which are critical aspects when considering the use of topographic derivates. Parameters such as flow direction and flow accumulation may not represent the complexity of flow patterns in IWP

315 terrain (e.g. Speetjens et al., 2024). Most models in our study did not consider elevation as important and other factors such as NDWI and vegetation height play a more important role for predicting SOC and N stock distribution. The models in our study only explain a fifth to a quarter of the spatial variability in SOC and N stocks. This suggest that to achieve high predictive power across this region, systematic additional soil sampling in addition to the compilation of local studies would be needed. A dataset that represents all landscape types, and predictors that co-vary with soil variability across space are needed.

320 **4.3   Comparing local scale results to regional scale synthesis**

Our study shows that the results of local studies can differ from the results in regional studies for the equivalent sub region. The two mainland sites Ptarmigan Bay and Komakuk Beach were studied on a high spatial resolution (2m) (Wagner et al., 2023) and SOC stocks were 40 kg C m^{-2} and 66.6 kg C m^{-2} respectively. The results of our study show 62 kg C m^{-2} and 47.8 kg C m^{-2} respectively with the entire area models and 63.5 kg C m^{-2} and 58.5 kg C m^{-2} with the mainland only models. For

325 Ptarmigan Bay, (Hugelius et al., 2013) suggest 92.8 kg C m^{-2} and (Mishra and Gautam, 2022) 63.4 kg C m^{-2}. At Komakuk Beach, (Hugelius et al., 2013) estimated 18.1 kg C m^{-2}. Furthermore, this synthesis shows that there are high local differences between different geographic areas when comparing different individual high resolution studies. In contrast, the results of the regional mapping lead to similar results for Komakuk Beach and Ptarmigan Bay. However, the SOC stocks for Komakuk Beach using the model with all data is significantly lower than using the mainland only model. This could be partially explained by the

330 inclusion of data from Herschel Island. Even though our study included more samples than Obu et al. (2017) and our methods differ (machine learning in contrast to class matching), average SOC stocks are similar in both studies. Obu et al. (2017) show 34.8 kg C m^{-2} for the upper metre of soil while our results show 36.2 kg C m^{-2} with the Herschel models and 41.9 kg C m^{-2} with the entire area models (Table 5). Large scale studies seemed to overpredict SOC stocks at Herschel Island. The estimated SOC stocks in the upper metre are according to Hugelius et al. (2013) 55.3 kg C m^{-2} at Herschel Island and 58.6 kg C m^{-2}

335 according to Mishra and Gautam (2022). For the mainland, Hugelius et al. (2013) provide an average of 64.5 kg C m^{-2} and Mishra and Gautam (2022) 52.8 kg C m^{-2}, though the latter does not account for the whole mainland area due to data gaps. Our study shows 57.1 kg C m^{-2} for the mainland, which lies in between the studies mentioned above.

    Our study underlines that large-scale studies should not just be split according to their geographic regions but also according to their geological identity. This is supported by the differences in important variables between different models. When using

340 all data together in one model, the elevation is the most important variable. For the mainland-only-model, the elevation was considered as less important while the NDWI was the most important variable. We also found that predictions of soil C and

N stocks vary significantly at different scales and with different data, and that models at larger scales can smooth out local variability. The dataset by Mishra and Gautam (2022) has a data gap at Komakuk Beach, west of Komakuk Beach and for a large portion of the area where DTLBs were sampled. This shows that the coastal area lacks accurate maps of SOC stocks.

345 Hence, our study contributes in complementing existing studies and provides moderate resolution datasets at regional scale. Furthermore, the fact that local SOC stocks can vary widely between studies needs to be taken into account in future carbon budget studies.

5 Conclusion

Our study synthesises existing soil data from different studies that have been carried out at the Yukon coastal plain, providing
350 an estimation of regional SOC and N stocks at 10 m spatial resolution for the top metre of soil. Furthermore, our study complements pan-Arctic estimates, especially as coastal areas are not well represented and there are large data gaps in pan-Arctic datasets. The average SOC stock for the upper metre for the entire area summing the results from the mainland and Herschel model is 56.7 ± 5.6 kg m^{-2} and the N stock 2.19 ± 0.51 kg m^{-2}. The values using all data are 44.7 ± 6.5 kg C m^{-2} and 1.81 ± 0.44 kg N m^{-2} respectively. We do not recommend using all data together, since the separate models for Herschel
355 Island and the mainland are likely more accurate. On Herschel Island the values are 36.2 ± 5.7 kg C m^{-2} and 2.66 ± 0.39 kg N m^{-2} respectively, at the mainland 57.2 ± 4.5 kg C m^{-2} and 2.17 ± 0.50 kg N m^{-2}.

Our study leads to several recommendations. First, we want to highlight that the usage/ exclusion of data might lead to very different model results, especially when extrapolating to areas with differences in geological genesis or soil parent material composition. We therefore recommend that pan-Arctic studies not only subdivide data into geographic regions, but also fol-
360 lowing landscape history. Second, we recommend the usage of the AOA to assess whether the relation between covariates and target variable is represented across the whole study area, as this approach can also help to determine new sampling sites. This requires additional spatial regional datasets that can be used as covariates that represent the soil forming factors. Third, we recommend using quantile regression forest to estimate the model uncertainty. Overall, we conclude that multi-scale studies are needed for better predictions of global soil C budgets in the wake of climate change, because they can provide a potent
365 bridge between high resolution local studies and moderate resolution pan-Arctic studies.

Data availability. The datasets and soil data will be made publicly available in the Bolin Centre Database: https://bolin.su.se/data/.

Author contributions. JW is the lead author and conceptualized the study, did the analysis and wrote a first draft. JWo provided new data-points that were not previously published and contributed text to the manuscript. AB provided remote sensing datasets and JR contributed soil data from a previous study. All co-authors provided input to writing of the manuscript.

370   *Competing interests.*   The authors declare that they have no conflict of interest.

Acknowledgements.   The authors would like to thank George Tanski for help with coring during the Yukon Coast 2019 spring field campaign and Justin Lindemann for assistance in AWI laboratories. We thank the Yukon Territorial Government, the Yukon Parks office (Herschel Island Qikiqtaruk Territorial Park), Parks Canada office (Ivvavik National Park) and the Aurora Research Institute and Aurora College (ARI) in Inuvik, NT, for administrative and logistical support for our fieldwork.

375   *Funding.* This study is part of the Nunataryuk project, which received funding under the European Union's Horizon 2020 Research and Innovation Programme under grant agreement no. 773421. JWo was funded by German Research Foundation (DFG) grant no. DFG WO 2420/2-1. JR received additional funding from the Swedish Academy of Science (Formas) under the Grant FR-2021/0004.

References

Bartsch, A., Widhalm, B., and Pointner, G.: Vegetation height derived from Sentinel-1 and Sentinel-2 satellite data (2015-2018) for tundra regions [dataset]., 2019a.

Bartsch, A., Widhalm, B., Pointner, G., Ermokhina, K., Leibman, M., and Heim, B.: Landcover derived from Sentinel-1 and Sentinel-2 satellite data (2015-2018) for Subarctic and Arctic environments. Zentralanstalt für Meteorologie und Geodynamik, Wien, PANGAEA, https://doi.org/10.1594/PANGAEA.897916, 2019b.

Bartsch, A., Efimova, A., Widhalm, B., Muri, X., von Baeckmann, C., Bergstedt, H., Ermokhina, K., Hugelius, G., Heim, B., and Leibman, M.: Circumarctic land cover diversity considering wetness gradients, Hydrology and Earth System Sciences, 28, 2421–2481, https://doi.org/10.5194/hess-28-2421-2024, 2024.

Biskaborn, B. K., Smith, S. L., Noetzli, J., Matthes, H., Vieira, G., Streletskiy, D. A., Schoeneich, P., Romanovsky, V. E., Lewkowicz, A. G., Abramov, A., Allard, M., Boike, J., Cable, W. L., Christiansen, H. H., Delaloye, R., Diekmann, B., Drozdov, D., Etzelmüller, B., Grosse, G., Guglielmin, M., Ingeman-Nielsen, T., Isaksen, K., Ishikawa, M., Johansson, M., Johannsson, H., Joo, A., Kaverin, D., Kholodov, A., Konstantinov, P., Kröger, T., Lambiel, C., Lanckman, J. P., Luo, D., Malkova, G., Meiklejohn, I., Moskalenko, N., Oliva, M., Phillips, M., Ramos, M., Sannel, A. B. K., Sergeev, D., Seybold, C., Skryabin, P., Vasiliev, A., Wu, Q., Yoshikawa, K., Zheleznyak, M., and Lantuit, H.: Permafrost is warming at a global scale, Nature Communications, 10, 1–11, https://doi.org/10.1038/s41467-018-08240-4, 2019.

Breiman, L.: Bagging predictors, Machine Learning, 24, 123–140, https://doi.org/10.1007/bf00058655, 1996.

Breiman, L.: Random Forests, Machine Learning, 45, 5–32, https://doi.org/https://doi.org/10.1023/A:1010933404324, 2001.

Burn, C. R.: Herschel Island: Qikiqtaryuk: A Natural Cultural History of Yukon's Arctic Island, Calgary, AB: University of Calgary Press, Calgary, Alberta, 1st editio edn., 2012.

Couture, N., Irrgang, A. M., Pollard, W. H., Lantuit, H., and Fritz, M.: Soil organic carbon (SOC) and sediment contents and fluxes for terrain units along the Yukon Coastal Plain, Canada, including corrections for volumetric ground ice contents [dataset, https://doi.org/https://doi.pangaea.de/10.1594/PANGAEA.884689, 2018a.

Couture, N. J. and Pollard, W. H.: A Model for Quantifying Ground-Ice Volume, Yukon Coast, Western Arctic Canada, Permafrost and Periglacial Processes, 28, 534–542, https://doi.org/10.1002/ppp.1952, 2017.

Couture, N. J., Irrgang, A., Pollard, W., Lantuit, H., and Fritz, M.: Coastal Erosion of Permafrost Soils Along the Yukon Coastal Plain and Fluxes of Organic Carbon to the Canadian Beaufort Sea, Journal of Geophysical Research: Biogeosciences, https://doi.org/10.1002/2017JG004166, 2018b.

ESRI: Esri. "World terrain base" [basemap], https://www.arcgis.com/home/item.html?id=33064a20de0c48d2bb61efa8faca93a8, accessed: 2024-07-04, 2024a.

ESRI: Esri. "World Hillshade" [basemap], https://www.arcgis.com/home/item.html?id=1b243539f4514b6ba35e7d995890db1d, accessed: 2025-03-05, 2024b.

Fritz, M., Wetterich, S., Meyer, H., Schirrmeister, L., Lantuit, H., and Pollard, W. H.: Origin and characteristics of massive ground ice on Herschel Island (western Canadian Arctic) as revealed by stable water isotope and Hydrochemical signatures, Permafrost and Periglacial Processes, 22, 26–38, https://doi.org/10.1002/ppp.714, 2011.

Fritz, M., Wetterich, S., Schirrmeister, L., Meyer, H., Lantuit, H., Preusser, F., and Pollard, W. H.: Eastern Beringia and beyond: Late Wisconsinan and Holocene landscape dynamics along the Yukon Coastal Plain, Canada, Palaeogeography, Palaeoclimatology, Palaeoecology, 319-320, 28–45, https://doi.org/10.1016/j.palaeo.2011.12.015, 2012.

415   Fritz, M., Wolter, J., Rudaya, N., Palagushkina, O., Nazarova, L., Obu, J., Rethemeyer, J., Lantuit, H., and Wetterich, S.: Holocene ice-wedge polygon development in northern Yukon permafrost peatlands (Canada), Quaternary Science Reviews, 147, 279–297, https://doi.org/10.1016/j.quascirev.2016.02.008, 2016.

Government of Canada: Canadian Climate Normals and Averages, http://climate.weather.gc.ca/climate_normals/index_e.html, http://climate. weather.gc.ca/climate_normals/index_e.html, accessed: 2024-05-25, 2024.

420   Hengl, T., de Jesus, J. M., Heuvelink, G. B. M., Gonzalez, M. R., Kilibarda, M., Blagotić, A., Shangguan, W., Wright, M. N., Geng, X., Bauer-Marschallinger, B., Guevara, M. A., Vargas, R., MacMillan, R. A., Batjes, N. H., Leenaars, J. G. B., Ribeiro, E., Wheeler, I., Mantel, S., and Kempen, B.: SoilGrids250m: Global gridded soil information based on machine learning, PloS one, 12, e0169 748, https://doi.org/10.1371/journal.pone.0169748, 2017.

Hugelius, G., Bockheim, J. G., Camill, P., Elberling, B., Grosse, G., Harden, J. W., Johnson, K., Jorgenson, T., Koven, C. D., Kuhry, P.,

425   Michaelson, G., Mishra, U., Palmtag, J., O'Donnell, J., Schirrmeister, L., Schuur, E. A., Sheng, Y., Smith, L. C., Strauss, J., and Yu, Z.: A new data set for estimating organic carbon storage to 3 m depth in soils of the northern circumpolar permafrost region, Earth System Science Data, 5, 393–402, https://doi.org/10.5194/essd-5-393-2013, 2013.

Hugelius, G., Strauss, J., Zubrzycki, S., Harden, J. W., Schuur, E. A. G., Ping, C.-L., Schirrmeister, L., Grosse, G., Michaelson, G. J., Koven, C. D., O'Donnell, J. A., Elberling, B., Mishra, U., Camill, P., Yu, Z., Palmtag, J., and Kuhry, P.: Estimated stocks of circumpolar permafrost

430   carbon with quantified uncertainty ranges and identified data gaps, Biogeosciences, 11, 6573–6593, https://doi.org/10.5194/bg-11-6573-2014, 2014.

Irrgang, A. M., Lantuit, H., Manson, G. K., Günther, F., Grosse, G., and Overduin, P. P.: Variability in Rates of Coastal Change Along the Yukon Coast, 1951 to 2015, Journal of Geophysical Research: Earth Surface, 123, 779–800, https://doi.org/10.1002/2017JF004326, 2018.

Kuhn, M.: Building Predictive Models in R Using the caret Package, Journal of Statistical Software, 28, https://doi.org/10.18637/jss.v028.i05,

435   2008.

Kuhn, M.: caret: Classification and Regression Training. R package version 6.0-92, 2022.

Kursa, M. B. and Rudnicki, W. R.: Feature selection with the boruta package, Journal of Statistical Software, 36, 1–13, https://doi.org/10.18637/jss.v036.i11, 2010.

Lagacherie, P.: Digital soil mapping: A state of the art, pp. 3–14, Springer Netherlands, ISBN 9781402085918, https://doi.org/10.1007/978-

440   1-4020-8592-5_1, 2008.

Lantuit, H. and Pollard, W. H.: Fifty years of coastal erosion and retrogressive thaw slump activity on Herschel Island, southern Beaufort Sea, Yukon Territory, Canada, Geomorphology, 95, 84–102, https://doi.org/10.1016/j.geomorph.2006.07.040, 2008.

Lantuit, H., Overduin, P. P., Couture, N., Wetterich, S., Aré, F., Atkinson, D., Brown, J., Cherkashov, G., Drozdov, D., Forbes, L. D., Graves-Gaylord, A., Grigoriev, M., Hubberten, H. W., Jordan, J., Jorgenson, T., Ødegård, R. S., Ogorodov, S., Pollard, W. H., Rachold, V.,

445   Sedenko, S., Solomon, S., Steenhuisen, F., Streletskaya, I., and Vasiliev, A.: The Arctic Coastal Dynamics Database: A New Classification Scheme and Statistics on Arctic Permafrost Coastlines, Estuaries and Coasts, 35, 383–400, https://doi.org/10.1007/s12237-010-9362-6, 2012.

Liaw, A. and Wiener, M.: Classifcation and Regression by randomForest, R News, 2(3), 18–22, https://cran.r-project.org/doc/Rnews/, 2002.

McBratney, A. B., Santos, M. L. M., and Minasny, B.: On digital soil mapping, Geoderma, 117, 3–52, https://doi.org/10.1016/S0016-

450   7061(03)00223-4, 2003.

Meredith, M., Sommerkorn, M., Cassotta, S., Derksen, C., Ekaykin, A., Hollo, A., Kofinas, G., Mackintosh, A., Melbourne-Thomas, J., Muelbert, M. M., Ottersen, G., Pritchard, H., and Schuur, E. A.: Polar Regions, pp. 203–320, Cambridge University Press, https://doi.org/10.1017/9781009157964.005, 2022.

Meyer, H. and Pebesma, E.: Predicting into unknown space? Estimating the area of applicability of spatial prediction models, Methods in
455 Ecology and Evolution, 12, 1620–1633, https://doi.org/10.1111/2041-210X.13650, 2021.

Meyer, H. and Pebesma, E.: Machine learning-based global maps of ecological variables and the challenge of assessing them, Nature Communications, 13, 1–4, https://doi.org/10.1038/s41467-022-29838-9, 2022.

Meyer, H., Ludwig, M., Milà, C., Linnenbrink, J., and Schumacher, F.: The CAST package for training and assessment of spatial prediction models in R. Url: http://arxiv.org/abs/2404.06978, http://arxiv.org/abs/2404.06978, 2024.

460 Mishra, U. and Gautam, S.: Spatial heterogeneity and environmental predictors of permafrost region soil organic carbon stocks [Dataset], https://datadryad.org/stash/dataset/doi:10.7941/D1GD1H, accessed: 2024-07-10, 2022.

Mishra, U., Hugelius, G., Shelef, E., Yang, Y., Strauss, J., Lupachev, A., Harden, J. W., Jastrow, J. D., Ping, C. L., Riley, W. J., Schuur, E. A. G., Matamala, R., Siewert, M., Nave, L. E., Koven, C. D., Fuchs, M., Palmtag, J., Kuhry, P., Treat, C. C., Zubrzycki, S., Hoffman, F. M., Elberling, B., Camill, P., Veremeeva, A., and Orr, A.: Spatial heterogeneity and environmental predictors of permafrost region soil
465 organic carbon stocks, Science Advances, 7, https://doi.org/10.1126/sciadv.aaz5236, 2021.

Obu, J.: How Much of the Earth's Surface is Underlain by Permafrost?, Journal of Geophysical Research: Earth Surface, 126, 1–5, https://doi.org/10.1029/2021JF006123, 2021.

Obu, J., Lantuit, H., Myers-Smith, I. H., Heim, B., Wolter, J., and Fritz, M.: Permafrost cores and active layer pits on Herschel Island: link to shape files, https://doi.org/https://doi.pangaea.de/10.1594/PANGAEA.859661, 2016.

470 Obu, J., Lantuit, H., Myers-Smith, I., Heim, B., Wolter, J., and Fritz, M.: Effect of Terrain Characteristics on Soil Organic Carbon and Total Nitrogen Stocks in Soils of Herschel Island, Western Canadian Arctic, Permafrost and Periglacial Processes, 28, 92–107, https://doi.org/10.1002/ppp.1881, 2017.

Obu, J., Westermann, S., Bartsch, A., Berdnikov, N., Christiansen, H. H., Dashtseren, A., Delaloye, R., Elberling, B., Etzelmüller, B., Kholodov, A., Khomutov, A., Kääb, A., Leibman, M. O., Lewkowicz, A. G., Panda, S. K., Romanovsky, V., Way, R. G., Westergaard-
475 Nielsen, A., Wu, T., Yamkhin, J., and Zou, D.: Northern Hemisphere permafrost map based on TTOP modelling for 2000–2016 at 1km2 scale, https://doi.org/10.1016/j.earscirev.2019.04.023, 2019.

Palmtag, J. and Kuhry, P.: Grain size controls on cryoturbation and soil organic carbon density in permafrost-affected soils, Permafrost and Periglacial Processes, 29, 112–120, https://doi.org/10.1002/ppp.1975, 2018.

Palmtag, J., Cable, S., Christiansen, H. H., Hugelius, G., and Kuhry, P.: Landform partitioning and estimates of deep storage of soil organic
480 matter in Zackenberg, Greenland, Cryosphere, 12, 1735–1744, https://doi.org/10.5194/tc-12-1735-2018, 2018.

Porter, C., Morin, P., Howat, I., Noh, M., Bates, B., Peterman, K., Keesey, S., Schlenk, M., Gardiner, J., Tomko, K., Willis, M., Kelleher, C., Cloutier, M., Husby, E., Foga, S., Nakamura, H., Platson, M., Wethington, M. J., Williamson, C., Bauer, G., Enos, J., Arnold, G., Kramer, W., Becker, P., Doshi, A., D'Souza, C., Cummens, P., Laurier, F., and Bojesen, M.: "ArcticDEM", https://doi.org/10.7910/DVN/OHHUKH, Harvard Dataverse, V1, [accessed on 10 January 2024]., 2018.

485 R Development Core Team: R: A language and environment for statistical computing. R Foundation for Statistical Computing, Vienna, Austria. ISBN 3-900051-07-0, URL http://www.R-project.org (12.08.2017)., 2021.

Ramage, J. L., Fortier, D., Hugelius, G., Lantuit, H., and Morgenstern, A.: Distribution of carbon and nitrogen along hillslopes in three valleys on Herschel Island, Yukon Territory, Canada, Catena, 178, 132–140, https://doi.org/10.1016/j.catena.2019.02.029, 2019.

Rampton, V. R.: Surficial geology, Yukon Coastal Plain, https://doi.org/10.4095/126954, 1982.

490 Rantanen, M., Karpechko, A. Y., Lipponen, A., Nordling, K., Hyvärinen, O., Ruosteenoja, K., Vihma, T., and Laaksonen, A.: The Arctic has warmed nearly four times faster than the globe since 1979, Communications Earth and Environment, 3, 1–10, https://doi.org/10.1038/s43247-022-00498-3, 2022.

Schuur, E. A. G., McGuire, A. D., Schädel, C., Grosse, G., Harden, J. W., Hayes, D. J., Hugelius, G., Koven, C. D., Kuhry, P., Lawrence, D. M., Natali, S. M., Olefeldt, D., Romanovsky, V. E., Schaefer, K., Turetsky, M. R., Treat, C. C., and Vonk, J. E.: Climate change and the

495 permafrost carbon feedback, Nature, 520, 171–179, https://doi.org/10.1038/nature14338, 2015.

Siewert, M. B.: High-resolution digital mapping of soil organic carbon in permafrost terrain using machine learning: A case study in a sub-Arctic peatland environment, Biogeosciences, 15, 1663–1682, https://doi.org/10.5194/bg-15-1663-2018, 2018.

Siewert, M. B., Hanisch, J., Weiss, N., Kuhry, P., Maximov, T. C., and Hugelius, G.: Comparing carbon storage of Siberian tundra and taiga permafrost ecosystems at very high spatial resolution, Journal of Geophysical Research: Biogeosciences, 120, 1973–1994,

500 https://doi.org/10.1002/2015JG002999, 2015.

Siewert, M. B., Hugelius, G., Heim, B., and Faucherre, S.: Landscape controls and vertical variability of soil organic carbon storage in permafrost-affected soils of the Lena River Delta, Catena, 147, 725–741, https://doi.org/10.1016/j.catena.2016.07.048, 2016.

Siewert, M. B., Lantuit, H., Richter, A., and Hugelius, G.: Permafrost Causes Unique Fine-Scale Spatial Variability Across Tundra Soils, Global Biogeochemical Cycles, 35, e2020GB006 659, https://doi.org/10.1029/2020GB006659, 2021a.

505 Siewert, M. B., Lantuit, H., Richter, A., and Hugelius, G.: Soil organic carbon, active layer depth and visible ground ice content for Herschel Island (Qikiqtaruk), https://doi.org/https://doi.pangaea.de/10.1594/PANGAEA.927861, 2021b.

Speetjens, N. J., Berghuijs, W. R., Wagner, J., and Vonk, J. E.: Degradation of ice-wedge polygons leads to increased fluxes of water and DOC, Science of The Total Environment, 920, 170 931, https://doi.org/10.1016/j.scitotenv.2024.170931, 2024.

Strauss, J., Abbott, B. W., Hugelius, G., Schuur, E., Treat, C., Fuchs, M., Schädel, C., Ulrich, M., Turetsky, M., Keuschnig, M., Biasi, C.,

510 Yang, Y., and Grosse, G.: 9. Permafrost. In: Recarbonizing global soils – A technical manual of recommended management practices, pp. 127 – 147, FAO, https://www.fao.org/publications/card/en/c/CB6378EN/, 2021.

Turetsky, M. R., Abbott, B. W., Jones, M. C., Anthony, K. W., Olefeldt, D., Schuur, E. A. G., Grosse, G., Kuhry, P., Hugelius, G., Koven, C., Lawrence, D. M., Gibson, C., Sannel, A. B. K., and McGuire, A. D.: Carbon release through abrupt permafrost thaw, Nature Geoscience, 13, 138–143, https://doi.org/10.1038/s41561-019-0526-0, 2020.

515 Virkkala, A. M., Niittynen, P., Kemppinen, J., Marushchak, M. E., Voigt, C., Hensgens, G., Kerttula, J., Happonen, K., Tyystjärvi, V., Biasi, C., Hultman, J., Rinne, J., and Luoto, M.: High-resolution spatial patterns and drivers of terrestrial ecosystem carbon dioxide, methane, and nitrous oxide fluxes in the tundra, Biogeosciences, 21, 335–355, https://doi.org/10.5194/bg-21-335-2024, 2024.

Wagner, J., Martin, V., Speetjens, N. J., A'Campo, W., Durstewitz, L., Lodi, R., Fritz, M., Tanski, G., Vonk, J. E., Richter, A., Bartsch, A., Lantuit, H., and Hugelius, G.: High resolution mapping shows differences in soil carbon and nitrogen stocks in areas of varying landscape

520 history in Canadian lowland tundra, Geoderma, 438, 116 652, https://doi.org/10.1016/j.geoderma.2023.116652, 2023.

Wagner, J., Martin, V. S., Speetjens, N. J., A'Campo, W., Durstewitz, L., Lodi, R., Fritz, M., Tanski, G., Vonk, J. E., Richter, A., Bartsch, A., Lantuit, H., and Hugelius, G.: High resolution datasets of soil organic carbon and nitrogen stocks in Canadian lowland tundra. Dataset version 1. Bolin Centre Database., 2024.

Walker, D. A., Reynolds, M. K., Daniëls, F. J., Einarsson, E., Elvebakk, A., Gould, W. A., Katenin, A. E., Kholod, S. S., Markon, C. J.,

525 Melnikov, E. S., Moskalenko, N. G., Talbot, S. S., Yurtsev, B. A., Bliss, L. C., Edlund, S. A., Zoltai, S. C., Wilhelm, M., Bay, C., Gudjónsson, G., Moskalenko, N. G., Ananjeva, G. V., Drozdov, D. S., Konchenko, L. A., Korostelev, Y. V., Melnikov, E. S., Ponomareva,

O. E., Matveyeva, N. V., Safranova, I. N., Shelkunova, R., Polezhaev, A. N., Johansen, B. E., Maier, H. A., Murray, D. F., Fleming, M. D., Trahan, N. G., Charron, T. M., Lauritzen, S. M., and Vairin, B. A.: The Circumpolar Arctic vegetation map, Journal of Vegetation Science, 16, 267–282, https://doi.org/10.1111/j.1654-1103.2005.tb02365.x, 2005.

530 Widhalm, B., Bartsch, A., and Goler, R.: Normalized C-HH backscatter from Sentinel-1 (December, 2014-2017) for selected tundra regions, https://doi.org/10.1594/PANGAEA.897046, supplement to: Widhalm, B et al. (2018): Simplified normalization of C-Band synthetic aperture radar data for terrestrial applications in high latitude environments. Remote Sensing, 10(4), 551, https://doi.org/10.3390/rs10040551, 2019.

Wolter, J., Lantuit, H., Fritz, M., Macias-Fauria, M., Myers-Smith, I., and Herzschuh, U.: Vegetation composition and shrub extent on the

535 Yukon coast, Canada, are strongly linked to ice-wedge polygon degradation, https://doi.org/10.3402/polar.v35.27489, 2016.

Wolter, J., Lantuit, H., Wetterich, S., Rethemeyer, J., and Fritz, M.: Climatic, geomorphologic and hydrologic perturbations as drivers for mid- to late Holocene development of ice-wedge polygons in the western Canadian Arctic, Permafrost and Periglacial Processes, 29, 164–181, https://doi.org/10.1002/ppp.1977, 2018.

Wolter, J., Jones, B. M., Fuchs, M., Breen, A., Bussmann, I., Koch, B., Lenz, J., Myers-Smith, I. H., Sachs, T., Strauss, J., Nitze, I., and

540 Grosse, G.: Post-drainage vegetation, microtopography and organic matter in Arctic drained lake basins, Environmental Research Letters, 19, 045 001, https://doi.org/10.1088/1748-9326/ad2eeb, 2024.

Yigini, Y., Olmedo, G., Reiter, S., Baritz, R., Viatkin, K., and Vargas, R.: Soil Organic Carbon Mapping Cookbook 2nd edition, FAO, 2018.